THE JOURNAL OF BIOLOGICAL CHEMISTRY VOL. 287, NO. 29, pp. 24228–24238, July 13, 2012

Mechanism for p38α-mediated Experimental Autoimmune Encephalomyelitis*[S]

Received for publication, December 30, 2011, and in revised form, May 21, 2012 Published, JBC Papers in Press, May 25, 2012, DOI 10.1074/jbc.M111.338541

Kana Namiki[‡], Hirofumi Matsunaga[‡§], Kento Yoshioka[‡], Kensuke Tanaka[‡], Kazuya Murata[¶], Junji Ishida[¶], Akira Sakairi[¶], Jundal Kim[¶], Naoki Tokuhara[‡], Nobuhiko Shibakawa[§], Motohisa Shimizu[§], Yukinori Wada[§], Yasunori Tokunaga[§], Manabu Shigetomi[§], Masahiko Hagihara[§], Sadao Kimura[‡], Tatsuhiko Sudo[‖], Akiyoshi Fukamizu[¶], and Yoshitoshi Kasuya[‡1]

From the [‡]Department of Biochemistry and Molecular Pharmacology, Graduate School of Medicine, Chiba University, Chiba 260-8670, the [§]Pharmaceuticals Research Laboratory, Ube Industries, Ltd., Ube 755-8633, the [¶]Life Science Center, Tsukuba Advanced Research Alliance, Graduate School of Life and Environmental Sciences, University of Tsukuba, Tennoudai, Ibaraki 305-8577, and the [‖]Chemical Biology Core Facility and Antibiotics Laboratory, RIKEN Advanced Science Institute, Wako, Saitama 3510198, Japan

Background: p38 signaling pathway plays a key role in inflammatory diseases.
Results: A single copy disruption of the *p38α* gene or a p38α inhibitor markedly reduced the pathogenesis of EAE by decreasing IL-17 production.
Conclusion: p38α regulates the pathogenesis of EAE through transcriptional regulation of IL-17 production.
Significance: Anti-p38α strategy achieves therapeutic benefit for the treatment of multiple sclerosis.

One of the mitogen-activated protein kinases, p38, has been found to play a crucial role in various inflammatory responses. In this study, we analyzed the roles of p38α in multiple sclerosis, using an animal model, experimental autoimmune encephalomyelitis (EAE). p38α$^{+/-}$ mice (p38α$^{-/-}$ showed embryonic lethality) showed less severe neurological signs than WT mice. Adoptive transfer of lymph node cells (LNC) from sensitized WT mice with MOG(35–55) to naive WT-induced EAE was much more severe compared with the case using LNC from sensitized p38α$^{+/-}$ mice. Comprehensive analysis of cytokines from MOG(35–55)-challenged LNC by Western blot array revealed that production of IL-17 was significantly reduced by a single copy disruption of the *p38α* gene or a p38 inhibitor. Likewise, by a luciferase reporter assay, an electrophoresis mobility shift assay, and characterization of the relationship between p38 activity and IL-17 mRNA expression, we confirmed that p38 positively regulates transcription of the *Il17* gene. Furthermore, oral administration of a highly specific p38α inhibitor (UR-5269) to WT mice at the onset of EAE markedly suppressed the progression of EAE compared with a vehicle group. These results suggest that p38α participates in the pathogenesis of EAE through IL-17 induction.

Multiple sclerosis (MS)[2] is an inflammatory autoimmune demyelinating disease of the central nervous system (CNS) that causes progressive decline of motor and sensory function and permanent disability (1). The mechanism of MS has often been studied using an animal model, EAE, that resembles the pathology of human MS (2). It is thought to be mediated in part by myelin-specific lymphocytes, and it shows infiltration of activated peripheral inflammatory cells into the CNS, attack of myelin by the immune system or cell death of oligodendrocytes, and axonal damage (3–5). Hence, to better understand the mechanism of the signs of EAE, EAE is characterized into two phases, an immune-mediated process and a neurodegenerative process (1). On the basis of this approach to EAE, various different classes of immunomodulatory agents have been discovered and approved for MS treatment (6).

MS was initially considered a T helper (Th)1 cell-dependent disease because of the correlation between disease severity and the expression levels of Th1 cytokines such as IFN-γ and IL-12 in peripheral blood mononuclear cells and cerebrospinal fluid (7, 8). However, mice with IFN-γ gene disruption develop EAE to a greater degree compared with WT mice (9). There is recent evidence that Th17 cells characterized by the production of IL-17 are involved in various autoimmune diseases and that IL-17 is the main mediator in EAE and MS (10, 11). Production of IL-17 by T cells is known to be dependent on IL-23, a heterodimeric cytokine composed of an IL-23-specific p19 subunit and a p40 subunit, shared with IL-12 (12, 13). p19- and p40-deficient mice are both resistant to actively induced EAE (14). In contrast, the lack of p35, an IL-12-specific subunit forming a heterodimer with p40, causes worsening of EAE, although p35-deficient mice show loss of function of IL-12 in inducing IFN-γ (15).

* This work was supported in part by Grants-in-aid for Scientific Research (B) 21390172 (to Y. K.) and Young Scientists (B) 20790201 (to K. N.) from the Ministry of Education, Science, Sports and Culture of Japan.
[S] This article contains supplemental Figs. S1–S5.
[1] To whom correspondence should be addressed: Dept. of Biochemistry and Molecular Pharmacology, Graduate School of Medicine, Chiba University, 1-8-1 Inohana, Chuo-ku, Chiba 260-8670, Japan. Tel.: 81-43-226-2193; Fax. 81-43-226-2196; E-mail: kasuya@faculty.chiba-u.jp.
[2] The abbreviations used are: MS, multiple sclerosis; p38, p38 mitogen-activated protein kinase; EAE, experimental autoimmune encephalomyelitis; LNC, lymph node cell; SC, spinal cord; MOG, myelin oligodendrocyte glycoprotein; PTX, pertussis toxin; CRE, cAMP-responsive element; CREB, CRE-binding protein; ATF, activating transcriptional factor; ANOVA, analysis of variance; dpi, days post-immunization; Tricine, *N*-[2-hydroxy-1,1-bis(hydroxymethyl)ethyl]glycine; c.a., constitutively active.

It is known that mitogen-activated protein kinases (MAPKs) transduce a variety of extracellular signals to the transcriptional machinery via a cascade of protein phosphorylation. There are three genetically distinct MAPKs in mammals, consisting of extracellular signal-regulated kinase (ERK), c-Jun N-terminal kinase (JNK), and p38 MAPK. All three members are activated by dual phosphorylation of the conserved T*X*Y motif and then phosphorylate their respective substrates on serine or threonine residues (16).

There are four mammalian isoforms of p38 (α, β, γ, and δ). p38α and -β are expressed ubiquitously in adult tissues (17), whereas p38γ is expressed predominantly in skeletal muscle (18), and p38δ has high levels of expression in the kidney and lung (19). The p38 signaling pathway is related to various diseases, including inflammatory diseases (20). Although *p38α* gene deficiency results in lethality in homozygous embryonic mice because of defects in erythropoiesis and placental organogenesis (21, 22), the p38$\alpha^{+/-}$ mouse is a useful tool for studying the *in vivo* role of p38α in certain disease models (23–27). By virtue of the p38$\alpha^{+/-}$ mouse, we have previously demonstrated that p38α can participate in both delayed-type hypersensitivity (23) and neurodegenerative disorder (27), suggesting the possibility that p38α could regulate the pathogenesis of neuroinflammation like EAE. In fact, it has been recently reported that inhibition of the p38 signaling pathway can affect IL-17 production by CD4 T cells (28, 29). In addition, it has been demonstrated that ASK1, one of the MAPK kinase kinases, regulates the severity of EAE through p38 activation (30).

Here, we showed that p38α signaling plays a crucial role in actively and passively induced EAE. Comprehensive analysis of cytokines from antigen-challenged LNC revealed that production of IL-17 is significantly reduced by a single copy disruption of the *p38α* gene. Likewise, activation of p38 in T cells regulates the production of IL-17 at the transcriptional level through the cAMP-responsive element (CRE), which is known as the binding site for activating transcriptional factor (ATF) 2. We also showed that oral administration of UR-5269, a p38 inhibitor highly specific for p38α, to MOG(35–55)-immunized mice showing clinical symptoms markedly suppresses the progression of EAE.

EXPERIMENTAL PROCEDURES

Experimental Animals—All animal procedures conformed to the Japanese regulations for animal care and use, following the Guidelines for Animal Experimentation of the Japanese Association for Laboratory of Animal Science, and were approved by the Animal Care and Use Committee of RIKEN and Chiba University. Male mice heterozygous for targeted disruption of the p38α gene (22) were crossed with C57BL/6J male mice (Saitama Experimental Animal Supply Co.) to generate p38$\alpha^{+/-}$ and p38$\alpha^{+/+}$ (wild type (WT)) mice. Offspring (>8 generations) were genotyped by PCR analysis of tail-derived DNA. Multiplex PCR with three primers per reaction was used. The primers were as follows: A, 5′-CCCTATACTCCCTCTCTGTGTAACTTTTG-3′; B, 5′-CCCAAACCCCAGAAAGAAATGATG-3′; and C, 5′-TTCAGTGACAACGTCGAGCACAGCTG-3′. Using these primers for one cycle at 94 °C for 5 min followed by 35 cycles at 94 °C for 30 s, 55 °C for 30 s, and 72 °C for 1 min, with an extension step of 7 min at 72 °C at the end of the last cycle, produced 800- and 450-bp fragments from the mutant and WT alleles, respectively. WT and p38$\alpha^{+/-}$ littermates aged 8–12 weeks were used for each experiment.

MOG Peptide—A synthetic peptide derived from myelin-oligodendrocyte-glycoprotein sequence 35–55 (MEVGWYRSPFSRVVHLYRNGK, MOG(35–55)) was synthesized by TORAY Research Center, Inc. (Tokyo).

Induction and Assessment of EAE—For the induction of EAE, mice were immunized subcutaneously in the four flanks with 100 μg of MOG(35–55) emulsified 1:1 in complete Freund's adjuvant (Difco) supplemented with 500 μg of *Mycobacterium tuberculosis* H37Ra on day 0. In addition, 120 ng of pertussis toxin (PTX; List Biological Laboratories, Campbell, CA) was injected intravenously on days 0 and 2. Mice were weighed and observed for signs of EAE daily. Scoring was as follows: 0, no disease; 0.5, partial tail paralysis; 1, complete tail paralysis; 1.5, decline in righting reflex; 2, impairment of righting reflex; 2.5, hindlimb weakness; 3, paralysis of one hindlimb; 3.5, paralysis of both hindlimbs; 4, paralysis of one forelimb; 4.5, paralysis of both forelimbs; 5; moribund or dead. To determine the effect of a p38 inhibitor on actively induced EAE, UR-5269 (4-(2-aminopyridin-4-yl)-3-(4-fluorophenyl)-1-(1,4,5,6-tetrahydro-6-oxopyridazin-3-yl)-1*H*-pyrazole methanesulfonate, International Publication Number WO2004029043) was used. Each mouse received daily oral administration of UR-5269 (30 mg/kg) just after showing partial tail paralysis (score, 0.5).

Histological Analysis—Mice were anesthetized with pentobarbital and perfused with ice-cold phosphate-buffered saline (PBS) followed by 4% paraformaldehyde. The spinal cord (SC) was dissected out and fixed in 4% paraformaldehyde. Paraffin-embedded sections were stained by Kluver-Barrera's method (Luxol fast blue/Nissl staining) for visualization of demyelination and neuronal loss and hematoxylin-eosin (HE) for visualization of inflammatory infiltrate. The degree of demyelination was scored as follows: 0, no demyelination; 1, mild demyelination; 2, moderate demyelination; 3, severe demyelination. Leukocytic infiltration was quantified as the percentage of the total SC area using Macromax MVC-DU (GOKO, Kanagawa, Japan).

Induction of Passive EAE—Mice were immunized with MOG(35–55) according to the method used for EAE induction without PTX injection. This procedure was used for preparation of LNC. A single cell suspension of LNC was prepared from mice at 10 days post-immunization (dpi) and stimulated with 20 μg/ml MOG(35–55) and 10 ng/ml mouse IL-23 (Biolegend, San Diego) in RPMI 1640 medium (Sigma) supplemented with 10% FBS, 500 μM 2-mercaptoethanol, penicillin (100 units/ml), and streptomycin (100 μg/ml) at 37 °C in a humidified atmosphere (5% CO_2). After 5 days of culture, the cells were collected and transferred intravenously into naive WT mice (5×10^7 cells per mouse). In addition, 120 ng of PTX was also injected intravenously into the mice on the day of transfer and on day 2. Mice were weighed and observed for signs of EAE daily.

Cytokine Production Assay—LNC were harvested from axillary, inguinal, and cervical lymph nodes of mice at 8 dpi. A single cell suspension of LNC was stimulated with 20 μg/ml MOG(35–55) or 2 μg/ml anti-mouse CD3 antibody (BD Biosciences) plus anti-mouse CD28 antibody (Biolegend) for 72 h.

The resulting supernatants were subjected to Mouse Cytokine Antibody Array 2 (RayBiotech Inc., Norcross, GA) detecting 32 cytokines and ELISA for IL-17 (Biolegend) according to each manufacturer's protocol. To detect the effect of a p38 inhibitor on IL-17 production from WT-LNC, the cells were incubated with MOG(35–55) or anti-mouse CD3 antibody plus anti-mouse CD28 antibody in the presence of 0.3 μM SB203580 or 0.3 μM UR-5269 for 72 h. Then the resulting supernatants were subjected to ELISA for IL-17.

Intracellular Cytokine Staining—A single cell suspension of LNC from mice at 8 dpi was stimulated with 20 μg/ml MOG(35–55) or 2 μg/ml anti-mouse CD3 antibody (BD Biosciences) plus anti-mouse CD28 antibody (Biolegend) for 2 days. Monensin (2 μM, Sigma) was also added to the medium 6 h before collecting the cells. The resulting cells were stained with allophycocyanin-conjugated CD4 antibody (Biolegend). After fixing and permeabilizing (Fix/Perm buffer, Biolegend), the cells were further stained with phycoerythrin-conjugated anti-IL-17 antibody and FITC-conjugated anti-IFN-γ antibody (BD Biosciences). Analysis was performed with a FACSCalibur flow cytometer (BD Biosciences) and FlowJo software (Tree Star Inc., Ashland, OR).

Construction of Mouse Il17 Promoter in Luciferase Reporter Vector—To amplify the mouse Il17 proximal promoter region involving the cAMP-responsive element (CRE) (GenBank™ accession number, NC_000067 REGION: 20720986–20724577) and create an XhoI site and a BglII site at the 5′ and 3′ ends, respectively, two PCR primers were designed as follows: sense primer 5′-AAACTCGAGAAAGGGGTGGTTCT-GTGCTG-3′ and antisense primer 5′-AAAAGATCTCGTGT-GAGGGTGGATGAAGAG-3′. Genomic DNA prepared from the tail of a WT C57BL/6J mouse was used as a template for PCR amplification with KOD FX (TOYOBO, Osaka, Japan). The settings of the thermal cycler were 35 cycles of 15 s at 98 °C, 30 s at 55 °C, and 45 s at 68 °C. The amplified product (170 bp) was purified and digested with XhoI and BglII. Then the purified fragment was subcloned into the XhoI/BglII site of the pGV-B2 vector and sequenced. To create mutations in the CRE, we elongated the sense PCR primer as follows, 5′-AAACTCG-AGAAAGGGGTGGTTCTGTGCTAAACTCATTTGAG-3′. With this modified sense primer and the antisense primer described above, PCR amplification was performed, and its product was subcloned into the XhoI/BglII site of the pGV-B2 vector and sequenced.

Luciferase Assay—The construct, pGV-B2-IL-17-prom. or pGV-B2-IL-17-prom. mut., was transfected into Jurkat cells with Amaxa Nucleofector II (Lonza AG, Basel, Switzerland) according to the manufacturer's instructions. To specifically activate p38, a constitutive active form of MKK6 (MAPK kinase for p38) was expressed in the cells by co-transfection of pcDNA3-MKK6c.a. with Amaxa Nucleofector II. As a negative control for pcDNA3-MKK6c.a., mock-transfection was performed with pcDNA3 empty vector. To determine the effect of a p38 inhibitor, UR-5269 at concentrations of 1 and 10 μM was applied to the cells just after transfection. After a 24-h incubation, the cells were lysed in lysis buffer (25 mM Tris-HCl (pH 8.0), 2 mM DTT, 2 mM EDTA, 10% glycerol, 1% Triton X-100, 4 mM $MgCl_2$, 4 mM EGTA, 0.2 mM PMSF). An aliquot of lysate (20 μl) was mixed with 50 μl of substrate solution (20 mM Tricine, 1.07 mM $(MgCO_3)4Mg(OH)_2{\cdot}5H_2O$, 2.67 mM $MgSO_4$, 0.1 mM EDTA, 33.3 mM DTT, 270 μM coenzyme A, 470 μM luciferin, 530 μM ATP). Luciferase activity was measured using a Wallac 1420 ARVOsx multilabel counter (PerkinElmer Life Sciences). Luciferase activity was normalized for the amount of protein in each lysate using the Bradford technique. In case of elucidating the effect of p38α expression level on the *Il17* promoter activity, siRNA targeting for p38α (human *MAPK14*) or nontargeting siRNA obtained from Thermo Scientific (Waltham, MA) was transfected into Jurkat cells 48h before the co-transfection of pGV-B2-IL-17-prom. and pcDNA3-MKK6c.a.

Electrophoresis Mobility Shift Assay (EMSA)—Nuclear extracts were prepared from Jurkat cells transfected with or without pcDNA3-MKK6c.a. In brief, the cells were suspended in buffer A (10 mM HEPES (pH 7.9), 10 mM KCl, 0.1 mM EGTA, 0.1 mM EDTA, 1 mM DTT, 0.5 mM PMSF and 1% protease inhibitor mixture 2 (Sigma)) and left on ice for 15 min. Then 0.6% Nonidet P-40 was added to each sample and mixed well for 10 s by a Vortex mixer. After centrifugation, precipitations were washed twice with buffer A. The resulting precipitations were resuspended in buffer B (20 mM HEPES (pH 7.9), 400 mM NaCl, 1 mM EGTA, 1 mM EDTA, 1 mM DTT, 1 mM PMSF, and 1% protease inhibitor mixture 2) and gently rotated at 4 °C for 30 min. After centrifugation, the supernatants were used as nuclear extracts. EMSAs were performed according to the manufacturer's protocols of LightShift chemiluminescent EMSA kit (Thermo Scientific). Biotin 3′-end-labeled forward and reverse oligonucleotides of 5′-ctgtgcTGACCTCAtttgag-3′, corresponding to the −126/−107 mouse *Il17* promoter sequence (the CRE is shown in capital letters), were annealed and used as a probe. For competition experiments, nonlabeled WT probe or mutant probe (two mutations in the CRE as in the case of luciferase assay) was added to the reaction. In case of elucidating the effect of antibody for ATF2 or CREB on protein-probe complex formation, nuclear extracts were preincubated with rabbit anti-human ATF2 monoclonal antibody (Cell Signaling Technology, Inc., Danvers, MA) or rabbit anti-human CREB monoclonal antibody (Cell Signaling Technology, Inc.) for 1 h at 20 °C. As a control, normal rabbit IgG was preincubated with nuclear extracts.

Detection of IL-17 mRNA—LNC were harvested from axillary, inguinal, and cervical lymph nodes of WT mice at 8 dpi. A single cell suspension of LNC was stimulated with 20 μg/ml MOG(35–55) in the absence or presence of 1 μM SB203580 or 1 μM UR-5269 for 24 h. Total RNA was prepared from the cells using ISOGEN (Wako Chemicals, Tokyo) according to the manufacturer's instructions. Each RNA sample (20 ng) was subjected to a duplex real time RT-PCR using QuantiFast probe assays with detection kits for mouse IL-17A (Mm_Il17a_2_FAM) and mouse β-actin (Mm_Actb-_2_MAX) obtained from Qiagen (Hilden). For each sample, the differences in threshold cycles between mRNA levels of *Il17a* and *Actb* genes (Δ*Ct*) were detected, and a calibrated Δ*Ct* value (ΔΔ*Ct*) was analyzed. The obtained relative values were then expressed as fold induction over the negative control.

Effect of p38 on IL-17 mRNA Stability—LNC were harvested from axillary, inguinal, and cervical lymph nodes of naive WT

mice. A single cell suspension of LNC was subjected to collection of $CD4^+$ T cells according to the manufacturer's protocol (Miltenyi Biotec., Bergisch Gladbach). The cells were transferred onto a plate precoated with 5 μg/ml anti-mouse CD3 antibody (BD Biosciences) and incubated with 2 μg/ml anti-mouse CD28 (Biolegend), 10 μg/ml anti-mouse IFN-γ (BD Biosciences), 10 μg/ml anti-mouse IL-4 (BD Biosciences), 30 ng/ml IL-6, 20 ng/ml IL-23, and 1 ng/ml TGF-β for 4 days. After stimulating the cells with 5 ng/ml phorbol 12-myristate 13-acetate (Sigma) and 250 ng/ml ionomycin (Sigma) in the presence or absence of 1 μM UR-5269 for 30 min, 5 μg/ml actinomycin D was applied to the cells. Total RNA was prepared from the cells 30 min and 1 and 2 h after the treatment with actinomycin D. The expression level of IL-17 mRNA was determined as described under "Detection of IL-17 mRNA."

Statistics—Data are expressed as means ± S.E. Statistical analysis was conducted using the software GraphPad Prism (Version 4.0: GraphPad Software Inc., San Diego). Statistical significance was determined by Student's *t* test or analysis of variance (ANOVA) followed by Student's *t* test, and *p* values < 0.05 were considered significant.

RESULTS AND DISCUSSION

p38α$^{+/-}$ Mice Are Resistant to EAE—Numerous studies have demonstrated that p38 is possibly related to various pathophysiological processes such as inflammatory diseases and neurodegenerative diseases (31), suggesting a possible regulatory role of p38 in neuroinflammatory diseases. Recently, several groups reported a possible role of p38 in the pathogenesis of EAE as follows: a TLR-ASK1-p38 pathway in glial cells leads to chemokine release affecting leukocytic infiltration accompanied by severe EAE (30); activation of p38 in CD4 T cells contributes to EAE progression by controlling IL-17 production (32); p38β in concert with p38α participates in T cell receptor-mediated T cell proliferation, and its activity affects EAE progression (33). However, there is no evidence regarding a functional role of p38α in EAE. For instance, in rheumatoid arthritis, p38 isoforms show differential profiles of expression and activation, suggesting that each p38 isoform may share functions in the progression of rheumatoid arthritis (34). Likewise, inverse actions of p38α and -β have been suggested in cardiac hypertrophy under pressure overload (35). Besides p38α with its predominant expression, p38β and -δ also exist in T cells (19). Then in this study, we used the p38α$^{+/-}$ mouse to determine the *in vivo* role of p38α in EAE, because it is a useful tool for analyzing the *in vivo* role of p38 in disease models (23–27). WT and p38α$^{+/-}$ mice were immunized with MOG(35–55) and monitored up to day 40. As shown in Fig. 1*A*, p38α$^{+/-}$ mice showed less severe neurological signs than did WT mice at all time points. Clinical parameters in this and other experiments are summarized in Table 1. The mean maximum score of p38α$^{+/-}$ mice was significantly lower than that of WT mice, although there was no difference in the mean date of EAE onset between the two genotypes. Remarkably, the incidence of the disease in p38α$^{+/-}$ mice (40%) was much lower than that in WT mice (91%). This difference in incidence between the two genotypes closely reflected the clinical score. Even though it is limited to individuals showing neurological signs, the mean maximum clinical score of p38α$^{+/-}$ mice (2.9 ± 0.3) was significantly lower than that of WT mice (4.1 ± 0.2). We next examined histopathological features of SC with EAE. WT and p38α$^{+/-}$ mice showing neurological signs were subjected to histopathological analysis at 20 and 50 dpi as the acute phase

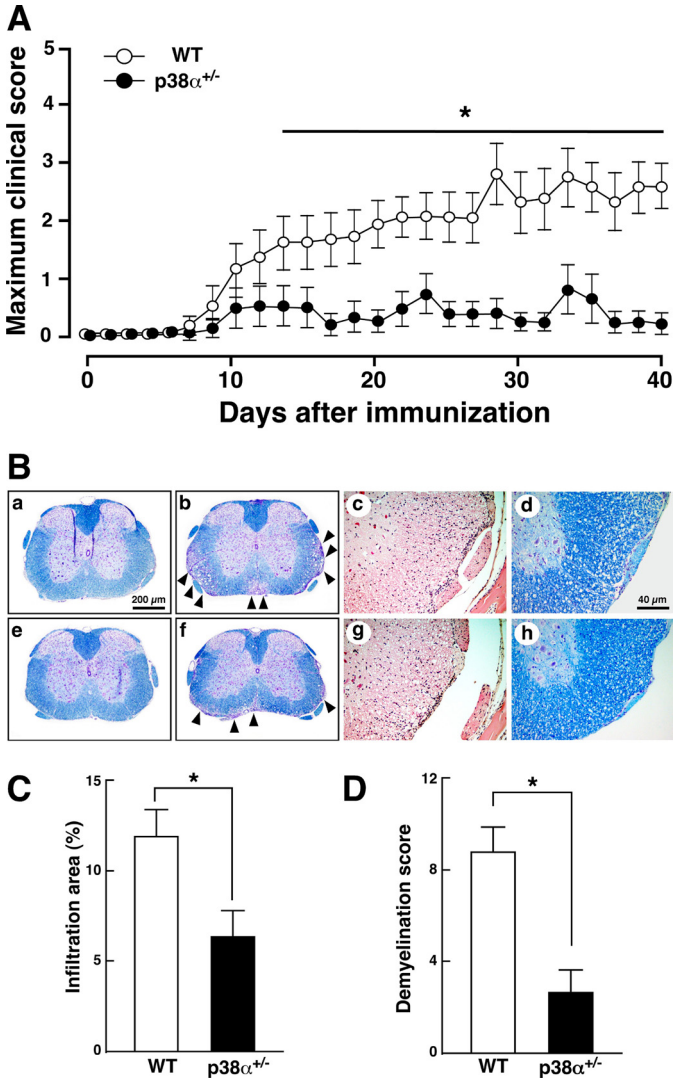

FIGURE 1. **Actively induced EAE.** *A,* clinical score of mice with MOG(35–55)-induced EAE. WT (*open circle*) and p38α$^{+/-}$ (*filled circle*) mice were immunized for EAE with MOG(35–55) emulsified in complete Freund's adjuvant and intravenously injected with PTX on days 0 and 2. They were monitored daily until day 40, and scoring was as described under "Experimental Procedures." Data represent mean ± S.E. The difference between the two groups at each time point was statistically significant (*, $p < 0.05$) as determined by Student's *t* test for unpaired values. *B,* histopathological findings in SC sections. Thoracic SC of WT (*panels a–c*) and p38α$^{+/-}$ mice (*panels e–g*) with sham-operation (*panels a* and *e*) or at 20 dpi (*panels b, c, f,* and *g*) were stained by Kluver-Barrera's method (*panels a, b, e,* and *f*) and with HE (*panels c* and *g*). Thoracic SC of WT (*panel d*) and p38α$^{+/-}$ mice (*panel h*) at 50 dpi were stained by Kluver-Barrera's method. The anterior funiculus area is shown at a higher magnification (*panels c, d, g,* and *h*). *Arrowheads* represent severe demyelination and vacuolation. *C,* leukocyte infiltration into SC of WT (*white bars*) and p38α$^{+/-}$ (*black bars*) mice. Data are shown as mean ± S.E. of six sections. The difference between the two groups was statistically significant (*, $p < 0.05$) as determined by Student's *t* test for unpaired values. *D,* demyelination score of WT (*white bars*) and p38α$^{+/-}$ (*black bars*) mice. Demyelination in the anterior, posterior, and both lateral funiculi (four areas) of each section was scored as described under "Experimental Procedures," and the scores were added together (maximum score = 12). Data are shown as mean ± S.E. of six sections. The difference between the two groups was statistically significant (*, $p < 0.05$) as determined by Student's *t* test for unpaired values.

TABLE 1
Clinical parameters of MOG(35–55)-induced EAE in WT and p38α$^{+/-}$ mice

Genotype	Incidence	Onset day ± S.E.	Maximum clinical score ± S.E. (individuals with onset)
WT	10/11	14.8 ± 1.1	3.7 ± 0.4 (4.1 ± 0.2)
p38α+/−	4/10	16.0 ± 1.2	1.2 ± 0.5[a] (2.9 ± 0.3[a])

[a] $p < 0.05$, significantly different from WT group by Student's *t* test. Data represent mean ± S.E.

and the chronic phase, respectively. In the acute phase, sections of the SC from WT mice revealed severe demyelination and vacuolation, which was reduced in the SC from p38α$^{+/-}$ mice (Fig. 1*B, panels a, b, e,* and *f*). The number of CNS inflammatory foci was decreased in p38α$^{+/-}$ mice compared with that in WT mice (Fig. 1*B, panels c* and *g*). Accordingly, in the chronic phase, demyelination and vacuolation were still apparent in the SC from WT mice compared with that in p38α$^{+/-}$ mice (Fig. 1*B, panels d* and *h*). Accordingly, the ratio of the leukocyte infiltration area to the whole SC area in the acute phase was significantly reduced in p38α$^{+/-}$ mice compared with that in WT mice (Fig. 1*C*). Semi-quantitative scoring of histological features revealed that the degree of demyelination in p38α$^{+/-}$ mice was significantly less than that in WT mice in the chronic phase (Fig. 1*D*). These findings clearly show that p38α$^{+/-}$ mice could be more resistant to MOG(35–55)-induced EAE compared with WT mice.

To elucidate the mechanisms underlying the attenuated signs of EAE in p38α$^{+/-}$ mice, differences in the potency of the immune responses to MOG(35–55) between p38α$^{+/-}$ and WT mice were examined in passively induced EAE. LNC from MOG(35–55)-immunized WT or p38α$^{+/-}$ mice were stimulated with MOG(35–55) and IL-23 for 5 days *in vitro*, and adoptively transferred into recipient naive mice with the same genetic background. As shown in Fig. 2, the development of EAE in mice receiving p38α$^{+/-}$ LNC was significantly reduced compared with that in those receiving WT LNC. Clinical parameters in this and other experiments are summarized in Table 2. The mean maximum score of mice receiving p38α$^{+/-}$ LNC was significantly lower than that of mice receiving WT LNC, and there is a difference in incidence between them. These results suggest that p38α in lymphocytes may at least contribute to the pathogenesis of EAE. Then the involvement of p38α in the production of key molecules for EAE from MOG(35–55)-immunized lymphocytes was investigated.

LNC-derived Cytokines Involved in EAE—Western blot array analysis of cytokine production in MOG(35–55)-stimulated LNC showed different expression patterns of several cytokines between the two genotypes (Fig. 3*A*). The correct location of each cytokine in the membrane is shown in supplemental Fig. S1. In LNC from MOG(35–55)-immunized WT mice, re-stimulation with MOG(35–55) induced IL-17, IFN-γ, and IL-3 expression and reduced MCP-1 expression compared with control. However, in LNC from MOG(35–55)-immunized p38α$^{+/-}$ mice, re-stimulation with MOG(35–55) induced IFN-γ expression and reduced MCP-1 expression. These results indicate that MOG(35–55)-induced IL-17 and IL-3 expressions were sensitive to p38α. Although little concerning the participation of IL-3 in EAE is known, a change in production of IL-3 in MOG-specific CD4 T cells is reported (36, 37). The induction ratio of signal to control revealed that MOG(35–55)-induced IL-17 expression was markedly suppressed in p38α$^{+/-}$ LNC compared with WT LNC. The induction ratio of IFN-γ by MOG(35–55) was not as high as that of IL-17 and showed no difference between the two genotypes (Fig. 3*B*). The quantitative detection of IL-17 by enzyme-linked immunosorbent assay (ELISA) was consistent with the results of Western blot array. However, the production of IL-17 from anti-CD3/CD28 Ab-activated LNC was not different between the two genotypes (Fig. 3*C*). These results suggest that p38α contributes to IL-17 production from antigen-specific effector T cells but not from T cells expanded through the antigen-presenting cell-free system. This notion was supported by flow cytometric analysis of intracellular IL-17 in CD4 T cells. Consistent with ELISA for IL-17, the frequency of CD4 T cells producing IL-17 in p38α$^{+/-}$ LNC was lower than that in WT LNC in the case of stimulation with MOG(35–55) but not anti-CD3/CD28 Abs (Fig. 3*D*). We also confirmed that the proliferation of antigen-specific LNC was consistent between the two genotypes, indicating that there is no impairment of activation of antigen-specific cells (data not shown).

Inhibitors of p38 have been actively developed as anti-inflammatory drugs (20, 31). UR-5269 is a newly discovered orally active compound that is highly specific for p38α (supplemental Fig. S2). Although SB203580 is occasionally used as a relative p38α-specific inhibitor (38), the specificity of UR-5269 for p38α *versus* -β is about two times higher than that of SB203580.

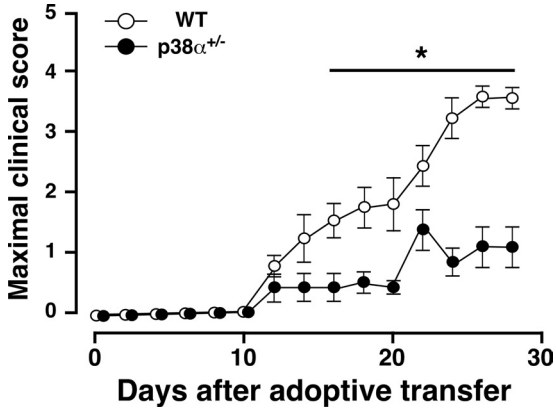

FIGURE 2. **Passively induced EAE.** The clinical score of naive WT mice after adoptive transfer of MOG(35–55)-stimulated LNC from WT (*white circles*) or p38α$^{+/-}$ (*black circles*) mice at 10 dpi. A single cell suspension of LNC from WT or p38α$^{+/-}$ mice at 10 dpi was stimulated *in vitro* with MOG(35–55) plus mouse IL-23. LNC with each genotype (5×10^7 cells/mouse) were adoptively transferred into naive WT mice intravenously, and mice were then injected with PTX on days 0 and 2 intravenously. The difference between the two groups was statistically significant (*, $p < 0.05$) as determined by Student's *t* test for unpaired values.

TABLE 2
Clinical parameters of passive EAE induced by LNC from MOG(35–55)-immunized WT and p38α$^{+/-}$ mice

Genotype of LNC	Incidence	Onset day ± S.E.	Maximum clinical score ± S.E.
WT	6/6	15.7 ± 2.4	3.8 ± 0.3
p38α+/−	3/6	15.3 ± 2.3	1.6 ± 0.7[a]

[a] $p < 0.05$, significantly different from WT group by Student's *t* test. Data represent mean ± S.E.

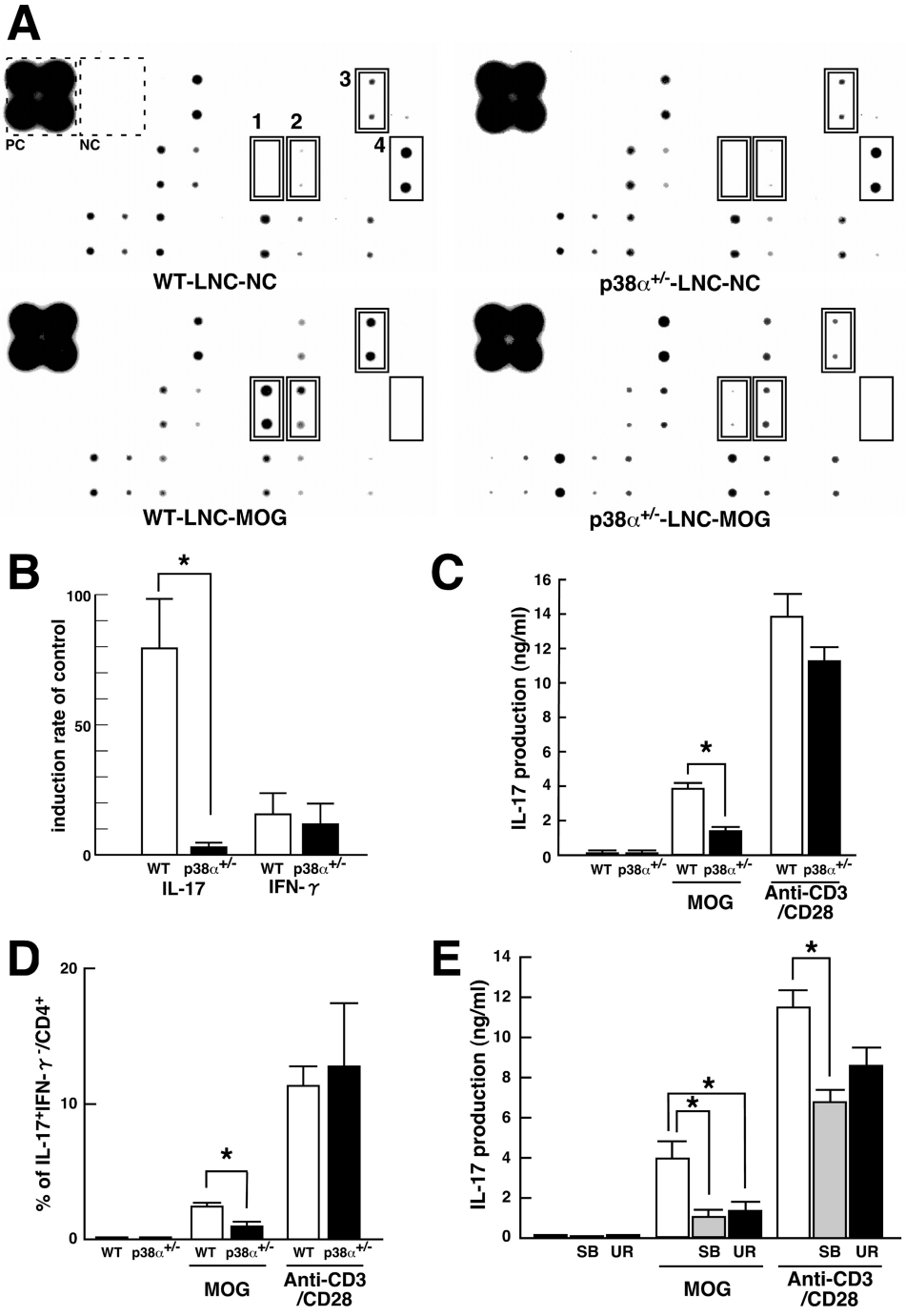

FIGURE 3. **Up-regulation of IL-17 in antigen-specific LNC mediated by p38α.** *A,* Western blot array analysis of cytokines from cultured LNC stimulated with MOG(35–55). LNC from WT and p38$\alpha^{+/-}$ mice at 8 dpi were stimulated *in vitro* with MOG(35–55) as an antigen-specific response. The supernatants were subjected to Mouse Cytokine Antibody Array 2. Compared with the unstimulated control, MOG(35–55)-induced and -reduced molecules are indicated by a *double-line* and a *single-line square*, respectively. Each *number* on the membrane represents the following: *1*, IL-17; *2*, IFN-γ; *3*, IL-3; and *4*, MCP-1. Positive and negative controls on the membrane in the reaction are indicated by a *dotted square*. *B,* change in expression of IL-17 and IFN-γ observed in Western blot array analyzed by densitometer. Each bar (*WT, white bars*; p38$\alpha^{+/-}$, *black bars*) is expressed as a percentage of the individual control signal without MOG(35–55) stimulation. Data are shown as mean ± S.E. ($n = 6$). The difference between the two groups was statistically significant (*, $p < 0.05$) as determined by Student's *t* test for unpaired values. *C,* MOG(35–55)-induced IL-17 in LNC. LNC from WT (*white bars*) and p38$\alpha^{+/-}$ (*black bars*) mice at 8 dpi were stimulated *in vitro* with MOG(35–55) as an antigen-specific response or anti-CD3/CD28 antibodies as an APC-free response. The resulting supernatants were subjected to ELISA for IL-17. Data are shown as means ± S.E. ($n = 4$). The difference between the two groups was statistically significant (*, $p < 0.05$) as determined by Student's *t* test for unpaired values. *D,* detection of IL-17-producing CD4 T cells by FACScan. LNC from WT (*white bars*) and p38$\alpha^{+/-}$ (*black bars*) mice at 8 dpi were stimulated *in vitro* with MOG(35–55) or anti-CD3/CD28 antibodies and subjected to surface staining for CD4 and intracellular staining for IL-17 and IFN-γ. Quantification of $CD4^+IL\text{-}17^+IFN\text{-}\gamma^-$ T cells was performed with FlowJo software. Data are shown as mean ± S.E. ($n = 4$). The difference between the two groups was statistically significant (*, $p < 0.05$) as determined by Student's *t* test for unpaired values. *E,* effects of p38 inhibitors on IL-17 production in LNC. LNC from WT mice at 8 dpi were stimulated *in vitro* with MOG(35–55) or anti-CD3/CD28 antibodies in the absence or presence of p38 inhibitor (SB203580 (*SB*), *shaded bars*; UR-5269 (*UR*), *black bars*). The resulting supernatants were subjected to ELISA for IL-17. Data are shown as mean ± S.E. ($n = 3$). *, $p < 0.05$, significantly different from the value without p38 inhibitors (*white bars*) (ANOVA with Bonferroni method).

Then, to further evaluate whether p38α contributes to IL-17 production from antigen-specific LNC, the effect of UR-5269 and SB203580 on MOG(35–55)-induced IL-17 production from WT LNC was determined. As expected, MOG(35–55)-induced IL-17 production was significantly inhibited by both SB203580 and UR-5269. However, anti-CD3/CD28 Ab-induced IL-17 production was reduced by SB203580 but not UR-5269 (Fig. 3*E*). Hence, at least for IL-17 production from LNC, the effect of UR-5269 mimicked the case with a single disruption of the *p38α* gene. Taking these results together, p38α can regulate IL-17 production in T cells.

IL-17 plays a key proinflammatory cytokine in a variety of inflammatory diseases (39). Correlation between induction of IL-17 and MS has been demonstrated in peripheral blood and the CNS (40, 41). Indeed, IL-17$^{-/-}$ mice show reduced clinical signs of EAE (10). Thus, p38α-regulated IL-17 production at least partly explains the mechanisms underlying the attenuated signs of EAE in p38$\alpha^{+/-}$ mice.

p38α Transcriptionally Regulates IL-17 Production—p38 phosphorylates and activates specific transcription factors such as ATF2, which forms homodimers as well as heterodimers with c-Jun or CREB and binds to the CRE (42–44). ATF2 can exhibit not only nuclear function but also cytoplasmic function, leading to a variety of regulatory roles in physiological and pathophysiological processes (45, 46). Especially in T lymphocytes, once stimulated with anti-CD3 antibody, CREB homodimer in the resting state is switched to form the CREB-ATF2 complex, which can strongly bind to CRE, indicating that ATF2 plays an important role during T lymphocyte activation and differentiation following engagement of the antigen receptor (47).

It has been clearly demonstrated that transactivation of the *IL17* promoter by the Tax protein, a *trans*-acting factor derived from human T cell leukemia virus type I, might be dependent on the CREB/ATF pathway and furthermore that the proximal promoter region of the *IL17* gene could be crucial in this step (48). We confirmed that the sequence of CRE (TGACCTCA corresponding to −119 to −112) is found in the promoter region of the mouse *Il17* gene (GenBank™ accession number NC_000067; Region 20720986–20724577) and that the sequence is conserved in various species (human, 48; rat, NC_005108, Region, 19454979–19458467; pig, NC_010449, Region, 52463736–52467313; cow, NC_007324, Region, 24931468–24934993). This element is not a typical palindromic consensus CRE (TGACGTCA) but is capable of binding to CREB/ATF proteins (49). Then we hypothesized that this region would be regulated by the p38/ATF2-signaling loop. To examine this hypothesis, we investigated the effect of p38 activation on luciferase reporter activity controlled by the *Il17* promoter in Jurkat cells. The sequence of the proximal promoter region of mouse *Il17* and sites of mutation produced in CRE are described in Fig. 4*A*. As shown in Fig. 4*B*, overexpression of a constitutively active mutant of MKK6 (MKK6c.a.) that specifically activates p38 significantly enhanced the reporter activity. This enhancement was significantly inhibited by treatment of the host cells with UR-5269 or by knockdown of p38α in the host cells. Likewise, mutation of the CREB/ATF-responsive element abolished the sensitivity of reporter activity to MKK6c.a. Under these experimental events, p38 possibly functions through regulating the activity of ATF2 and CREB (supplemental Fig. S3). The findings in the luciferase assay were supported by the results of EMSA. As shown in Fig. 4*C*, activation of p38 by the overexpression of MKK6c.a. induced the interaction between the proximal *Il17* promoter probe (−126/−107) and nuclear proteins as determined by the shifted band. This formation of the shifted band was inhibited by competition with excessive cold WT probe but not with excessive cold mutant probe possessing mutation of the CREB/ATF-responsive element. Moreover, preincubation of nuclear extracts with antibody for ATF2 or CREB abolished the formation of the same band. Thus, these results suggest that p38α up-regulates IL-17 production at the transcriptional level through the activation of ATF2/CREB binding to CRE in the *Il17* promoter region.

Recently, it has been demonstrated that p38 regulates IL-17 synthesis in CD4 T cells at a transcription-independent level through activation of the eukaryotic translation initiation factor 4E/MAPK interacting kinase (eIF-4E/MNK) pathway. In addition, IL-17 mRNA content was consistent in Th17-polarizing condition with or without SB203580 (32). However, this study clearly demonstrated that the transcriptional regulation of *Il17* by p38 might contribute to the pathogenesis of EAE. This finding probably reflects the induction of IL-17 mRNA under p38 activation in Th17-polarizing condition. Then we further elucidated this possibility. As we expected, the MOG(35–55)-induced IL-17 mRNA expression in LNC was markedly inhibited by both UR-5269 and SB203580 (Fig. 4*D*), indicating that the induction of IL-17 mRNA was regulated by p38. The post-transcriptional processes also regulate the expression level of mRNA. In fact, it is well known that p38 positively regulates the mRNA stability of cytokines (50). Then we also estimated whether p38 affects the stability of IL-17 mRNA. As shown in Fig. 4*E*, the half-life of IL-17 mRNA in Th17 cells was not decreased but rather increased by UR-5269. These results suggest that p38α might not up-regulate IL-17 mRNA through the induction of IL-17 mRNA stability.

We used MKK6c.a. to activate p38 for determination of the transcriptional regulation of IL-17 production. Activation of p38 by MKK is commonly recognized as the canonical pathway. As an alternative and stress-free pathway for activation of p38, phosphorylation on Tyr-323 by Zap70 has been identified in T cells (51). However, this ZAP70-mediated p38 activation pathway affects Th17 differentiation rather than IL-17 production from CD4 T cells in the pathogenesis of EAE (33). Hence, it is of interest that the manner of p38 activation in CD4 T cells has functional diversity. Also, our present study suggests that an anti-p38α strategy may have therapeutic benefit in MS. Then we elucidated the effect of UR-5269 on EAE susceptibility and severity.

UR-5269 Ameliorates EAE Progression—WT mice were immunized with MOG(35–55), and the onset of EAE was monitored. After determining the onset in each mouse (clinical score, 0.5), mice were randomly divided into two groups. One group received daily oral administration of UR-5269, and the control group received daily oral administration of vehicle (distilled water). Up to day 40, clinical signs and body weight were monitored. As shown in Fig. 5*A*, the cumulative clinical score of

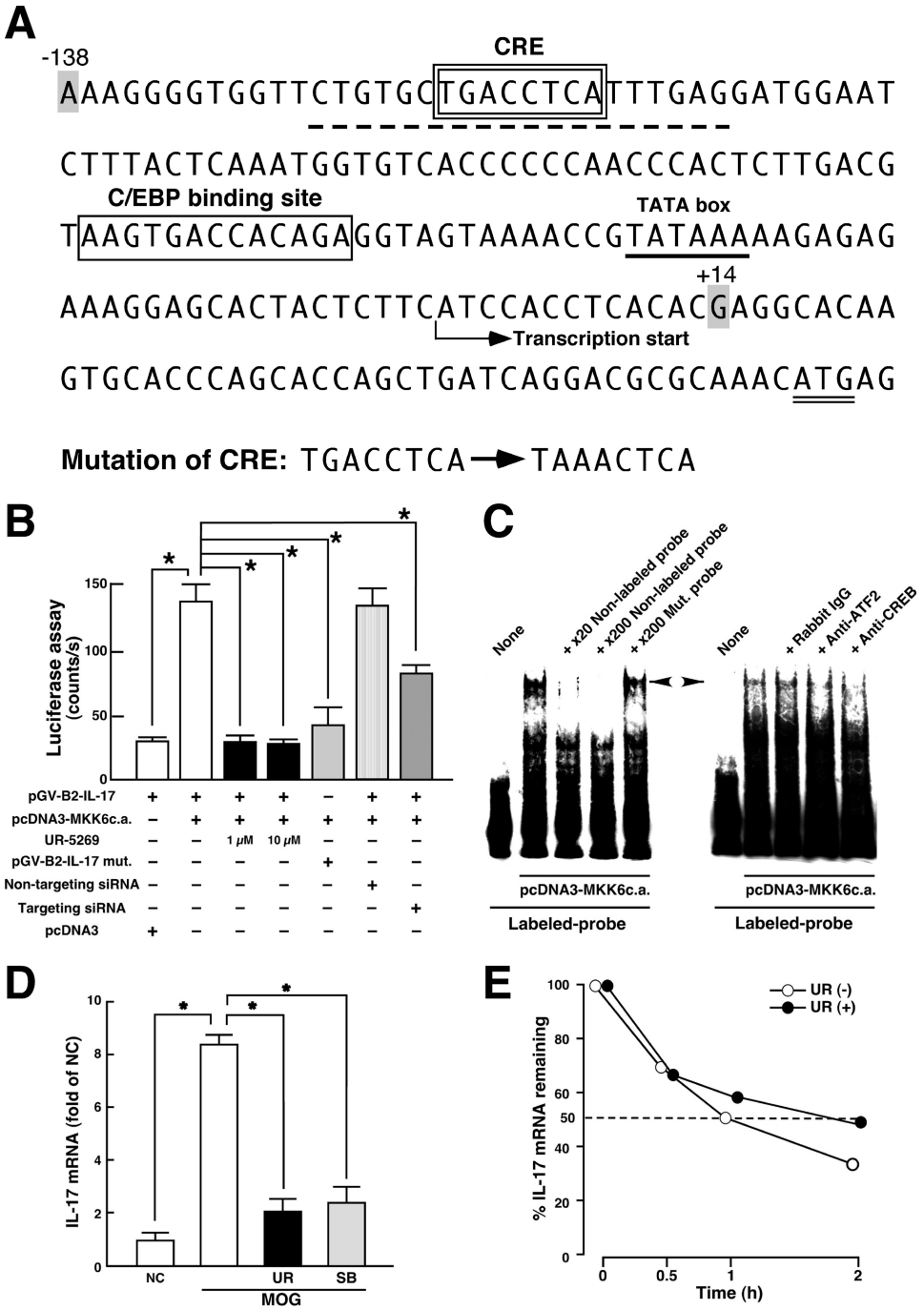

FIGURE 4. **Transcriptional regulation of IL-17 production by p38 pathway.** *A,* nucleotide sequence of 5′-flanking proximal region of mouse *Il17a* gene. CRE- and C/EBP-binding site are enclosed by a *double-line* and a *single-line square*, respectively. The TATA box (*underline*), initiation codon (*double underline*), probe sequence used in *C* (*dotted underline*), and transcriptional start site are indicated. The mutation sites produced in CRE are described. The region (−138/+14) of mouse *Il17a* gene was subcloned into pGV-B2 luciferase reporter vector. *B,* luciferase assay for p38 signal-dependent regulation of *Il17a* gene. Jurkat cells were transfected with the indicated expression plasmids. siRNAs were introduced into the cells 48 h before the transfection of plasmids. Cell lysates were subjected to luciferase assay 24 h after incubation. To determine the effect of UR-5269, incubation was performed in the presence of 1 or 10 μM UR-5269. Data are shown as mean ± S.E. ($n = 6$). *, $p < 0.05$, significantly different from stimulation value determined as co-transfection of pGV-B2-IL-17 and pcDNA3-MKK6c.a. (ANOVA with Bonferroni method). *C,* EMSA for p38-induced protein-probe complexes. Nuclear extracts were prepared from Jurkat cells transfected with pcDNA3-MKK6c.a. and subjected to interaction with labeled WT probe (*dotted underline* in *A*). Competition assays were performed by further adding 20- and 200-fold molar excess of unlabeled WT probe or 200-fold molar excess of unlabeled Mut. probe (mutation sites in the CRE as described in *A*). A *left-directed arrowhead* indicates specific band showing the protein complexes bound to the CRE in proximal promoter of *Il17* gene. A *right-directed arrowhead* indicates a disappeared band in EMSA when nuclear extracts were preincubated with either anti-ATF2 antibody or anti-CREB antibody. Similar results were obtained from three independent experiments. *D,* effect of p38 inhibitors on MOG(35–55)-induced IL-17 mRNA expression in LNC. LNC from WT mice at 8 dpi were stimulated *in vitro* with MOG(35–55) for 24 h in the absence or presence of p38 inhibitor (UR-5269 (*UR*), *black bars*; SB203580 (*SB*), *shaded bars*). Total RNA was subjected to a real time RT-PCR for IL-17. Signal values were normalized by the expression of β-actin and expressed as fold induction over the negative control (*NC*). Data are shown as mean ± S.E. ($n = 6$). *, $p < 0.05$, significantly different from stimulation value (ANOVA with Bonferroni method). *E,* effect of p38 on IL-17 mRNA stability. Th17 cells differentiated *in vitro* were stimulated with phorbol 12-myristate 13-acetate and ionomycin in the presence (*closed circle*) or absence (*open circle*) of 1 μM UR-5269 for 30 min, and then actinomycin D (5 μg/ml) was added for 0.5, 1, and 2 h. Total RNA was subjected to a real time RT-PCR for IL-17. Results are expressed as percentage of IL-17 mRNA remaining after normalized to β-actin. Means from two independent experiments are presented.

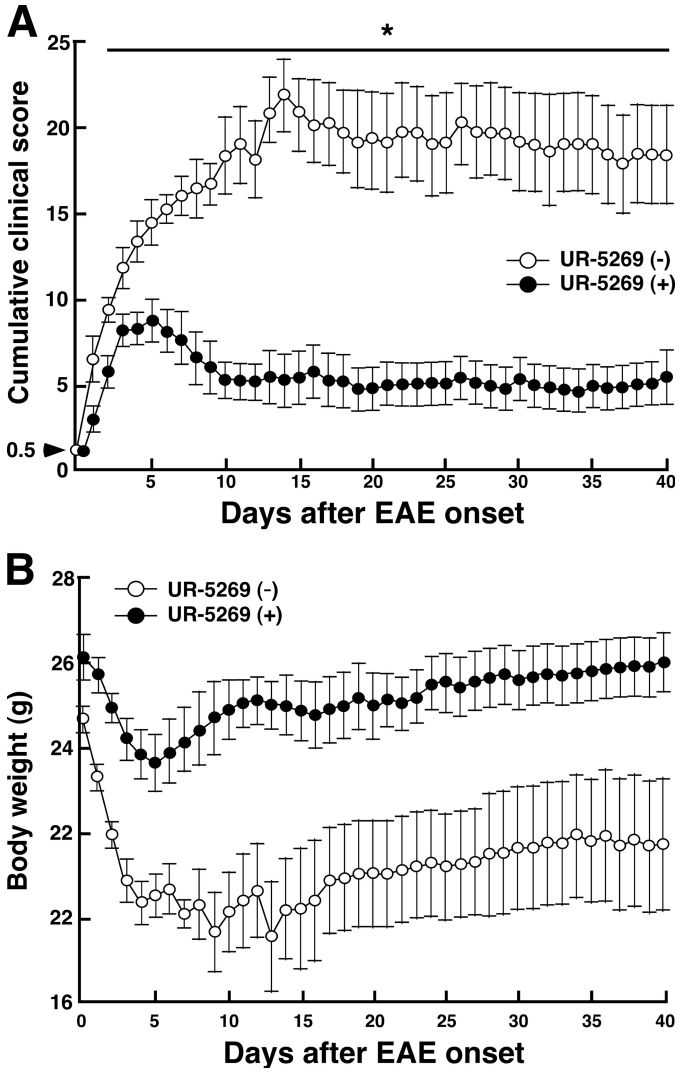

FIGURE 5. **Effect of UR-5269 on progression of EAE.** WT mice were immunized with MOG(35–55) to actively induce EAE and monitored. After determining the onset of EAE, mice immediately received oral daily administration of vehicle (*white circles*) or UR-5269 (30 mg/kg, *closed circles*). *A,* clinical score of mice with or without UR-5269 treatment. *B,* body weight of mice with or without UR-5269 treatment.

mice with UR-5269 treatment was markedly reduced at all times compared with that in control mice. Likewise, a significant beneficial effect of UR-5269 was observed 2 days after administration. Accordingly, body weight of mice with UR-5269 treatment tended to recover 5 days after onset. In contrast, body weight of control mice showed the lowest level at 13 days after onset and was thereafter maintained (Fig. 5*B*). These results suggest that inhibition of p38α by UR-5269 can ameliorate the progression of EAE even after its onset. We also evaluated the effect of another p38 inhibitor, SB239063, on actively induced EAE. It has been reported that SB239063, a second generation p38 inhibitor, has improved kinase selectivity and a potentiated anti-inflammatory effect compared with SB235080. In particular, SB239063 was found to effectively protect against CNS disorders such as brain injury (52). As expected, MOG(35–55)-immunized mice with oral daily administration of SB239063 just after showing partial tail paralysis (clinical score, 0.5) showed less severe development of EAE compared with the vehicle group (supplemental Fig. S4). However, its inhibitory effect was not as strong as that of UR-5269. Manifestation of a significant beneficial effect of SB239063 required a longer period of time compared with UR-5269.

We utilized p38α$^{+/-}$ mice and a highly p38α-specific inhibitor to elucidate how p38α regulates the pathogenesis of EAE. Both tools could bring the role of p38α in EAE into sharp relief. As one of the mechanisms of p38α-mediated EAE, transcriptional regulation of IL-17 production by p38α in antigen-specific T cells was demonstrated. Very recently, it has been demonstrated that p38α in dendritic cells but not macrophages or T cells can mediate the pathogenesis of EAE (53). However, an *in vitro* reconstitution model using CD4$^+$ T cells and CD11c$^+$ dendritic cells from the two genotypes suggests that the potency of MOG(35–55)-stimulated IL-17 production was attributed to the activity of p38α not in CD11c$^+$ dendritic but in CD4$^+$ T cells (supplemental Fig. S5). Although a possible explanation for the discrepancy is difficult, there may be a different output between the conditional knock-out system and the single disruption of the *p38α* gene. In this study, we also propose that an orally active and highly p38α-specific inhibitor, UR-5269, may have therapeutic benefits for the treatment of MS.

Acknowledgments—We thank Dr. Wendy Gray for editing this manuscript and Yasushi Konno for helpful discussion.

REFERENCES

1. Steinman, L. (2001) Multiple sclerosis. A two-stage disease. *Nat. Immunol.* **2,** 762–764
2. Taneja, V., and David, C. S. (2001) Lessons from animal models for human autoimmune diseases. *Nat. Immunol.* **2,** 781–784
3. Krishnamoorthy, G., Saxena, A., Mars, L. T., Domingues, H. S., Mentele, R., Ben-Nun, A., Lassmann, H., Dornmair, K., Kurschus, F. C., Liblau, R. S., and Wekerle, H. (2009) Myelin-specific T cells also recognize neuronal autoantigen in a transgenic mouse model of multiple sclerosis. *Nat. Med.* **15,** 626–632
4. Tokuhara, N., Namiki, K., Uesugi, M., Miyamoto, C., Ohgoh, M., Ido, K., Yoshinaga, T., Yamauchi, T., Kuromitsu, J., Kimura, S., Miyamoto, N., and Kasuya, Y. (2010) N-type calcium channel in the pathogenesis of experimental autoimmune encephalomyelitis. *J. Biol. Chem.* **285,** 33294–33306
5. Hisahara, S., Yuan, J., Momoi, T., Okano, H., and Miura, M. (2001) Caspase-11 mediates oligodendrocyte cell death and pathogenesis of autoimmune-mediated demyelination. *J. Exp. Med.* **193,** 111–122
6. Farooqi, N., Gran, B., and Constantinescu, C. S. (2010) Are current disease-modifying therapeutics in multiple sclerosis justified on the basis of studies in experimental autoimmune encephalomyelitis? *J. Neurochem.* **115,** 829–844
7. Moldovan, I. R., Rudick, R. A., Cotleur, A. C., Born, S. E., Lee, J. C., Karafa, M. T., and Pelfrey, C. M. (2003) Interferon γ responses to myelin peptides in multiple sclerosis correlate with a new clinical measure of disease progression. *J. Neuroimmunol.* **141,** 132–140
8. Fassbender, K., Ragoschke, A., Rossol, S., Schwartz, A., Mielke, O., Paulig, A., and Hennerici, M. (1998) Increased release of interleukin-12p40 in MS. Association with intracerebral inflammation. *Neurology* **51,** 753–758
9. Ferber, I. A., Brocke, S., Taylor-Edwards, C., Ridgway, W., Dinisco, C., Steinman, L., Dalton, D., and Fathman, C. G. (1996) Mice with a disrupted IFN-γ gene are susceptible to the induction of experimental autoimmune encephalomyelitis (EAE). *J. Immunol.* **156,** 5–7
10. Komiyama, Y., Nakae, S., Matsuki, T., Nambu, A., Ishigame, H., Kakuta, S., Sudo, K., and Iwakura, Y. (2006) IL-17 plays an important role in the development of experimental autoimmune encephalomyelitis. *J. Immu-*

nol. **177,** 566–573
11. Wang, H. H., Dai, Y. Q., Qiu, W., Lu, Z. Q., Peng, F. H., Wang, Y. G., Bao, J., Li, Y., and Hu, X. Q. (2011) Interleukin-17-secreting T cells in neuromyelitis optica and multiple sclerosis during relapse. *J. Clin. Neurosci.* **18,** 1313–1317
12. Langrish, C. L., Chen, Y., Blumenschein, W. M., Mattson, J., Basham, B., Sedgwick, J. D., McClanahan, T., Kastelein, R. A., and Cua, D. J. (2005) IL-23 drives a pathogenic T cell population that induces autoimmune inflammation. *J. Exp. Med.* **201,** 233–240
13. Oppmann, B., Lesley, R., Blom, B., Timans, J. C., Xu, Y., Hunte, B., Vega, F., Yu, N., Wang, J., Singh, K., Zonin, F., Vaisberg, E., Churakova, T., Liu, M., Gorman, D., Wagner, J., Zurawski, S., Liu, Y., Abrams, J. S., Moore, K. W., Rennick, D., de Waal-Malefyt, R., Hannum, C., Bazan, J. F., and Kastelein, R. A. (2000) Novel p19 protein engages IL-12p40 to form a cytokine, IL-23, with biological activities similar as well as distinct from IL-12. *Immunity* **13,** 715–725
14. Cua, D. J., Sherlock, J., Chen, Y., Murphy, C. A., Joyce, B., Seymour, B., Lucian, L., To, W., Kwan, S., Churakova, T., Zurawski, S., Wiekowski, M., Lira, S. A., Gorman, D., Kastelein, R. A., and Sedgwick, J. D. (2003) Interleukin-23 rather than interleukin-12 is the critical cytokine for autoimmune inflammation of the brain. *Nature* **421,** 744–748
15. Becher, B., Durell, B. G., and Noelle, R. J. (2002) Experimental autoimmune encephalitis and inflammation in the absence of interleukin-12. *J. Clin. Invest.* **110,** 493–497
16. Chang, L., and Karin, M. (2001) Mammalian MAP kinase signaling cascades. *Nature* **410,** 37–40
17. Jiang, Y., Chen, C., Li, Z., Guo, W., Gegner, J. A., Lin, S., and Han, J. (1996) Characterization of the structure and function of a new mitogen-activated protein kinase (p38β). *J. Biol. Chem.* **271,** 17920–17926
18. Li, Z., Jiang, Y., Ulevitch, R. J., and Han, J. (1996) The primary structure of p38γ. A new member of p38 group of MAP kinases. *Biochem. Biophys. Res. Commun.* **228,** 334–340
19. Jiang, Y., Gram, H., Zhao, M., New, L., Gu, J., Feng, L., Di Padova, F., Ulevitch, R. J, R., and Han, J. (1997) Characterization of the structure and function of the fourth member of p38 group mitogen-activated protein kinases, p38δ. *J. Biol. Chem.* **272,** 30122–30128
20. Kumar, S., Boehm, J., and Lee, J. C. (2003) p38 MAP kinases. Key signaling molecules as therapeutic targets for inflammatory diseases. *Nat. Rev. Drug Discov.* **2,** 717–726
21. Adams, R. H., Porras, A., Alonso, G., Jones, M., Vintersten, K., Panelli, S., Valladares, A., Perez, L., Klein, R., and Nebreda, A. R. (2000) Essential role of p38α MAP kinase in placental but not embryonic cardiovascular development. *Mol. Cell* **6,** 109–116
22. Tamura, K., Sudo, T., Senftleben, U., Dadak, A. M., Johnson, R., and Karin, M. (2000) Requirement for p38α in erythropoietin expression. A role for stress kinases in erythropoiesis. *Cell* **102,** 221–231
23. Takanami-Ohnishi, Y., Amano, S., Kimura, S., Asada, S., Utani, A., Maruyama, M., Osada, H., Tsunoda, H., Irukayama-Tomobe, Y., Goto, K., Karin, M., Sudo, T., and Kasuya, Y. (2002) Essential role of p38 mitogen-activated protein kinase in contact hypersensitivity. *J. Biol. Chem.* **277,** 37896–37903
24. Otsu, K., Yamashita, N., Nishida, K., Hirotani, S., Yamaguchi, O., Watanabe, T., Hikoso, S., Higuchi, Y., Matsumura, Y., Maruyama, M., Sudo, T., Osada, H., and Hori, M. (2003) Disruption of a single copy of the p38α MAP kinase gene leads to cardioprotection against ischemia-reperfusion. *Biochem. Biophys. Res. Commun.* **302,** 56–60
25. Sakurai, K., Matsuo, Y., Sudo, T., Takuwa, Y., Kimura, S., and Kasuya, Y. (2004) Role of p38 mitogen-activated protein kinase in thrombus formation. *J. Recept. Signal. Transduct. Res.* **24,** 283–296
26. Matsuo, Y., Amano, S., Furuya, M., Namiki, K., Sakurai, K., Nishiyama, M., Sudo, T., Tatsumi, K., Kuriyama, T., Kimura, S., and Kasuya, Y. (2006) Involvement of p38α mitogen-activated protein kinase in lung metastasis of tumor cells. *J. Biol. Chem.* **281,** 36767–36775
27. Namiki, K., Nakamura, A., Furuya, M., Mizuhashi, S., Matsuo, Y., Tokuhara, N., Sudo, T., Hama, H., Kuwaki, T., Yano, S., Kimura, S., and Kasuya, Y. (2007) Involvement of p38α in kainate-induced seizure and neuronal cell damage. *J. Recept. Signal. Transduct. Res.* **27,** 99–111
28. Lu, L., Wang, J., Zhang, F., Chai, Y., Brand, D., Wang, X., Horwitz, D. A., Shi, W., and Zheng, S. G. (2010) Role of SMAD and non-SMAD signals in the development of Th17 and regulatory T cells. *J. Immunol.* **184,** 4295–4306
29. Gulen, M. F., Kang, Z., Bulek, K., Youzhong, W., Kim, T. W., Chen, Y., Altuntas, C. Z., Sass Bak-Jensen, K., McGeachy, M. J., Do, J. S., Xiao, H., Delgoffe, G. M., Min, B., Powell, J. D., Tuohy, V. K., Cua, D. J., and Li, X. (2010) The receptor SIGIRR suppresses Th17 cell proliferation via inhibition of the interleukin-1 receptor pathway and mTOR kinase activation. *Immunity* **32,** 54–66
30. Guo, X., Harada, C., Namekata, K., Matsuzawa, A., Camps, M., Ji, H., Swinnen, D., Jorand-Lebrun, C., Muzerelle, M., Vitte, P. A., Rückle, T., Kimura, A., Kohyama, K., Matsumoto, Y., Ichijo, H., and Harada, T. (2010) Regulation of the severity of neuroinflammation and demyelination by TLR-ASK1-p38 pathway. *EMBO Mol. Med.* **12,** 504–515
31. Coulthard, L. R., White, D. E., Jones, D. L., McDermott, M. F., and Burchill, S. A. (2009) p38(MAPK). Stress responses from molecular mechanisms to therapeutics. *Trends Mol. Med.* **15,** 369–379
32. Noubade, R., Krementsov, D. N., Del Rio, R., Thornton, T., Nagaleekar, V., Saligrama, N., Spitzack, A., Spach, K., Sabio, G., Davis, R. J., Rincon, M., and Teuscher, C. (2011) Activation of p38 MAPK in CD4 T cells controls IL-17 production and autoimmune encephalomyelitis. *Blood* **118,** 3290–3300
33. Jirmanova, L., Giardino Torchia, M. L., Sarma, N. D., Mittelstadt, P. R., and Ashwell, J. D. (2011) Lack of the T cell-specific alternative p38 activation pathway reduces autoimmunity and inflammation. *Blood* **118,** 3280–3289
34. Korb, A., Tohidast-Akrad, M., Cetin, E., Axmann, R., Smolen, J., and Schett, G. (2006) Differential tissue expression and activation of p38 MAPK α, β, γ, and δ isoforms in rheumatoid arthritis. *Arthritis Rheum.* **54,** 2745–2756
35. Hirota, H., Chen, J., Betz, U. A., Rajewsky, K., Gu, Y., Ross, J., Jr., Müller, W., and Chien, K. R. (1999) Loss of a gp130 cardiac muscle cell survival pathway is a critical event in the onset of heart failure during biomechanical stress. *Cell* **97,** 189–198
36. Offner, H., Vainiene, M., Celnik, B., Weinberg, A. D., Buenafe, A., Vandenbark, A. A. (1994) Coculture of TCR peptide-specific T cells with basic protein-specific T cells inhibits proliferation, IL-3 mRNA, and transfer of experimental autoimmune encephalomyelitis. *J. Immunol.* **153,** 4988–4996
37. Hofstetter, H. H., Karulin, A. Y., Forsthuber, T. G., Ott, P. A., Tary-Lehmann, M., and Lehmann, P. V. (2005) The cytokine signature of MOG-specific CD4 cells in the EAE of C57BL/6 mice. *J. Neuroimmunol.* **170,** 105–114
38. Commodaro, A. G., Bombardieri, C. R., Peron, J. P., Saito, K. C., Guedes, P. M., Hamassaki, D. E., Belfort, R. N., Rizzo, L. V., Belfort, R., Jr., and de Camargo, M. M. (2010) p38α MAP kinase controls IL-17 synthesis in Vogt-Koyanagi-Harada syndrome and experimental autoimmune uveitis. *Invest. Ophthalmol. Vis. Sci.* **51,** 3567–3574
39. Weaver, C. T., Hatton, R. D., Mangan, P. R., and Harrington, L. E. (2007) IL-17 family cytokines and the expanding diversity of effector T cell lineages. *Annu. Rev. Immunol.* **25,** 821–852
40. Matusevicius, D., Kivisäkk, P., He, B., Kostulas, N., Ozenci, V., Fredrikson, S., and Link, H. (1999) Interleukin-17 mRNA expression in blood and CSF mononuclear cells is augmented in multiple sclerosis. *Mult. Scler.* **5,** 101–104
41. Lock, C., Hermans, G., Pedotti, R., Brendolan, A., Schadt, E., Garren, H., Langer-Gould, A., Strober, S., Cannella, B., Allard, J., Klonowski, P., Austin, A., Lad, N., Kaminski, N., Galli, S. J., Oksenberg, J. R., Raine, C. S., Heller R., and Steinman, L. (2002) Gene-microarray analysis of multiple sclerosis lesions yields new targets validated in autoimmune encephalomyelitis. *Nat. Med.* **8,** 500–508
42. Kyriakis, J. M., and Avruch, J. (2001) Mammalian mitogen-activated protein kinase signal transduction pathways activated by stress and inflammation. *Physiol. Rev.* **81,** 807–869
43. Hai, T., and Curran, T. (1991) Cross-family dimerization of transcription factors Fos/Jun and ATF/CREB alters DNA binding specificity. *Proc. Natl. Acad. Sci. U.S.A.* **88,** 3720–3724
44. Liu, H., Deng, X., Shyu, Y. J., Li, J. J., Taparowsky, E. J., and Hu, C. D. (2006)

Mutual regulation of c-Jun and ATF2 by transcriptional activation and subcellular localization. *EMBO J.* **25,** 1058–1069
45. Bhoumik, A., and Ronai, Z. (2008) ATF2. A transcription factor that elicits oncogenic or tumor suppressor activities. *Cell Cycle* **7,** 2341–2345
46. Lopez-Bergami, P., Lau, E., and Ronai, Z. (2010) Emerging roles of ATF2 and the dynamic AP1 network in cancer. *Nat. Rev. Cancer* **10,** 65–76
47. Feuerstein, N., Firestein, R., Aiyar, N., He, X., Murasko, D., and Cristofalo, V. (1996) Late induction of CREB/ATF binding and a concomitant increase in cAMP levels in T and B lymphocytes stimulated via the antigen receptor. *J. Immunol.* **156,** 4582–4593
48. Dodon, M. D., Li, Z., Hamaia, S., Gazzolo L. (2004) Tax protein of human T-cell leukemia virus type 1 induces interleukin 17 gene expression in T cells. *J. Gen. Virol.* **85,** 1921–1932
49. Merezak, C., Pierreux, C., Adam, E., Lemaigre, F., Rousseau, G. G., Calomme, C., Van Lint, C., Christophe, D., Kerkhofs, P., Burny, A., Kettmann, R., and Willems, L. (2001) Suboptimal enhancer sequences are required for efficient bovine leukemia virus propagation *in vivo.* Implications for viral latency. *J. Virol.* **75,** 6977–6988
50. Patil, C., Zhu, X., Rossa, C., Jr., Kim, Y. J., and Kirkwood, K. L. (2004) p38 MAPK regulates IL-1β-induced IL-6 expression through mRNA stability in osteoblasts. *Immunol. Invest.* **33,** 213–233
51. Ashwell, J. D. (2006) The many paths to p38 mitogen-activated protein kinase activation in the immune system. *Nat. Rev. Immunol.* **6,** 532–540
52. Barone, F. C., Irving, E. A., Ray, A. M., Lee, J. C., Kassis, S., Kumar, S., Badger, A. M., White, R. F., McVey, M. J., Legos, J. J., Erhardt, J. A., Nelson, A. H., Ohlstein, E. H., Hunter, A. J., Ward, K., Smith, B. R., Adams, J. L., and Parsons, A. A. (2001) SB 239063, a second-generation p38 mitogen-activated protein kinase inhibitor, reduces brain injury and neurological deficits in cerebral focal ischemia. *J. Pharmacol. Exp. Ther.* **296,** 312–321
53. Huang, G., Wang, Y., Vogel, P., Kanneganti, T. D., Otsu, K., and Chi, H. (2012) Signaling via the kinase p38α programs dendritic cells to drive TH17 differentiation and autoimmune inflammation. *Nat. Immunol.* **13,** 152–161